Quiescent Crystallization of Natural Fibers–Polypropylene Composites

Usa Somnuk,[1] Gerhard Eder,[2] Pranee Phinyocheep,[3] Nitinat Suppakarn,[1] Wimonlak Sutapun,[1] Yupaporn Ruksakulpiwat[1]

[1]*School of Polymer Engineering, Institute of Engineering, Suranaree University of Technology, Nakorn Ratchasima, Thailand*
[2]*Institute of Polymer Science, Johannes Kepler University, Linz, Austria*
[3]*Department of Chemistry, Faculty of Science, Mahidol University, Bangkok, Thailand*

Received 1 March 2007; accepted 20 May 2007
DOI 10.1002/app.26883
Published online 9 August 2007 in Wiley InterScience (www.interscience.wiley.com).

ABSTRACT: The effect of natural fibers (vetiver grass and rossells) on quiescent crystallization of polypropylene (PP) composites was analyzed in this study. Also, equilibrium melting temperature (T_m^0) of the composites was elucidated. Natural fiber-PP composites showed lower T_m^0 when compared to neat PP. Thermal analysis was performed via differential scanning calorimeter to study the crystallization kinetics. Natural fiber-PP composites exhibited higher rate of crystallization than that of neat PP. Furthermore, spherulitic growth rate and transcrystallinity of the composites were investigated under a polarized light optical microscope. It was found that the growth rates of the composites were lower than that of neat PP. The spherulitic growth rates combined with the crystallization rates were used to calculate number of effective nuclei. It was shown that the number of effective nuclei of the composites was higher than that of neat PP. This suggested that natural fibers could act as a nucleating agent in the composite. © 2007 Wiley Periodicals, Inc. J Appl Polym Sci 106: 2997–3006, 2007

Key words: crystallization; nucleation; polypropylene; composites; spherulites

INTRODUCTION

Polypropylene (PP) is one of the interesting commodity thermoplastics, because of its high isotacticity, high cost-performance ratio, and its low processing temperature. Therefore, its worldwide production grows up very fast during years and there are possibilities to modify PP to a wide range of final products for several kinds of applications. Thermal and mechanical properties of polymeric materials can be significantly improved using fillers.[1] In recent years, natural fibers have been increasingly used as alternative fillers in polymer composites.[2–5] Their advantages over synthetic fibers are low cost, less tool wear during processing, low density, environmental friendly, biodegradability, and renewability.[6–8] The natural fibers have potential to dramatically modify the crystallization characteristics of a given polymer matrix. The ultimate properties of the natural fiber–polymer composites depend on their microstructure and crystallinity. Additionally, the failure of the materials takes place at the microscopic level. Recently, several efforts have been made to characterize the effect of fibers, which served as fillers or reinforcements on crystallization of various thermoplastic polymers.[9–21] Experimental evidence confirms that the fibers affect the crystallization kinetics and morphology of the matrix. However, those studies have mentioned on the synthetic fibers[9–17] or inorganic fillers.[22–32]

In this study, natural fibers used for polymer composite are vetiver grass and rossells. Vetiver grass is a tropical plant, which well adapt to different environments. According to His Majesty the King Bhumipol Adulyadej of Thailand's Royal Initiative, the main purpose of vetiver grass cultivation is to conserve soil and water, particularly for the steep slope areas. Normally, leaves of the vetiver grass have been cut every few months to keep the vetiver rows in order. Only a minor portion of the residues is reserved as animal feed or household fuel. On the other hand, huge quantities of the remaining residues are burnt in fields or on the side of road. Rossells are planted tremendously in the northern part of Thailand. To help the farmer gain some extra income, our previous effort has been made to use vetiver grass and rossells as fillers in polymer composites.[5,33] It was found that PP composites from vetiver grass and rossells exhibited higher tensile strength, yield stress, and Young's modulus than that of neat PP. This indicated that both vetiver grass and rossells could serve as reinforcements in PP composites.

Correspondence to: Y. Ruksakulpiwat (yupa@sut.ac.th).
Contract grant sponsors: Thailand Research Fund (TRF) and Suranaree University of Technology.

Journal of Applied Polymer Science, Vol. 106, 2997–3006 (2007)

In the present work, the crystallization kinetics of vetiver grass-PP composites and rossells-PP composites were studied. The effect of vetiver grass and rossells on equilibrium melting temperature, half-time of crystallization, and crystallization rate of the composites were examined. The spherulitic growth rates of neat PP and PP composites were determined. In addition, nuclei concentration of the composites was explored.

EXPERIMENTAL

Materials

Vetiver grass and rossells were washed by water to eliminate dirt and dried in an oven at 100°C for 24 h. After that, they were prepared into a length of 2 mm. The aspect ratio of vetiver grass and rossells was 6.15 and 27.82, respectively. The vetiver grass was immersed in a solution of 4% (wt) NaOH for 2 h at 40°C and the vetiver-to-solution ratio is 1 : 25 (w/v). The vetiver grass was then washed by water and dried in an oven at 100°C for 24 h. The rossells fibers were treated as follows. The fibers were weighed about 700 g and put into a reactor. The 10 L methanol/benzene mixture (1 : 1) was then added into the reactor and heated to 80°C for 3 h. After that, the rossells fibers were immersed in 2% (wt) NaOH solution for 2 h at room temperature, subsequently washed by water, and then dried overnight in an oven at 100°C.

A commercial grade of isotactic PP (700J) supplied by Thai Polypropylene Co., Ltd. was mixed with each natural fiber in an internal mixer (model Hakke Rheomix Polylab) at 170°C. The ratio of natural fiber to PP is 20 : 80. Then, each composite sample was prepared into a thin film with a thickness of 50 μm using a compression molding.

Isothermal crystallization of natural fibers-PP composites

Thermal properties of PP composites were determined using a differential scanning calorimeter (DSC, Perkin–Elmer: model DSC7). The sample was heated from 25 to 200°C and held at 200°C for 5 min to eliminate the thermal history of sample. Then, the sample was cooled down with a rate of 40°C/min to various predetermined crystallization temperatures (T_c) and maintained at that temperature until the crystallization was completed. The enthalpy from DSC thermogram was used to obtain the relative degree of crystallinity, $X(t)$, by using the following equation.[29]

$$X(t) = \frac{\int_0^t (dH/dt)dt}{\int_0^\infty (dH/dt)dt} \quad (1)$$

where dH denotes the measured enthalpy of crystallization during an infinitesimal time interval dt. The limits t and ∞ are used to denote the elapsed time during the course of crystallization and at the end of the crystallization process, respectively.

After the crystallization completed, the samples were heated to the melting point at a rate of 10°C/min. The melting temperature (T_m) of the samples was obtained from the maximum of the endothermic peaks. The equilibrium melting temperatures (T_m^0) was determined from Hoffman-Weeks plot (the extrapolation plot of T_c versus T_m).[11]

Isothermal crystallization rate constant by Avrami plots

The relative degree of crystallinity, $X(t)$, is related to the crystallization time, t, according to Avrami equation as shown in the following equation[34–36]:

$$X(t) = 1 - \exp(-kt^n) \quad (2)$$

where n is the Avrami exponent which is a function of the nucleation process and k is the isothermal rate constant of crystallization. The values of n and k can be calculated by fitting to experimental data using the double logarithmic form as shown in eq. (3)

$$\log\{-\ln[1 - X(t)]\} = \log k + n \log t \quad (3)$$

A plot of $\log\{-\ln[1 - X(t)]\}$ as a function of $\log t$ yields a straight line with slope n and intercept $\log k$ called an Avrami plot.

Isothermal crystallization rate constant by half-time of crystallization

The half-time of crystallization, $t_{1/2}$, which is the elapsed time from the crystallization onset time until the relative degree of crystallinity reaches a values of 0.5, was determined and used to calculate the isothermal rate of crystallization from the following equation.[34–36]

$$k(T) = \frac{\ln 2}{(t_{1/2})^n} \quad (4)$$

where n is assumed to be 3.

Nonisothermal rate constant from isothermal experiment

Nonisothermal crystallization rate constant was obtained by using Nakamura expression[37,38]:

$$X(t) = 1 - \exp\left[-\int K(T)dt\right]^n \quad (5)$$

where $K(T)$ is nonisothermal crystallization rate constant which is related to the isothermal crystallization rate constant as shown in eq. (6).

$$K(T) = [k(T)]^{1/n} \tag{6}$$

The overall rate of nonisothermal crystallization

The nonisothermal rate constant $K(T)$, obtained from eq. (6), can be expressed by Hoffman-Lauritzen expression.[39]

$$K(T) = (\ln 2)^{1/n}\left(\frac{1}{t_{1/2}}\right)_0 \exp\left[\frac{-U^*}{R(T_c - T_\infty)}\right] \exp\left[\frac{-K_k}{T_c(\Delta T)f}\right] \tag{7}$$

From the expression, the kinetic model has four parameters: $\left(1/t_{1/2}\right)_0$ is the pre-exponential factor that includes all terms independent of temperature, K_k is the nucleation exponent, U^* and T_∞ are the Vogel-Fulcher-Tamman-Hesse (VFTH) parameters describing the transport of polymer segments across the liquid/crystal interphase, ΔT denotes the supercooling ($\Delta T = T_m^0 - T_c$) and $f = 2T_c/(T_c + T_m^0)$ is a correction factor accounting for the temperature dependence of the latent heat of fusion. R is the gas constant. The universal values used for the VFTH parameters are U^* = 1500 cal/mol (6280 J/mol) and $T_\infty = (T_g - 30)$ K.[29] In this study, the T_g value of PP was 270 K[40] and the equilibrium melting temperature, T_m^0, was obtained from this study.

Spherulitic growth rate and number of effective nuclei

Thin films (the thickness of 50 μm) of natural fibers-PP composites and neat PP were prepared by compression molding. Then, the samples were used to measure the spherulitic growth rate (G) by means of a Hot Stage (Linkam TH600) under a Polarized Optical Microscope connected with CCD video camcorder system (Sony). The sample was heated from room temperature to 200°C with a heating rate of 10°C/min and held at that temperature for 5 min. Then, the sample was cooled down with a rate of 50°C/min to various T_c. The radius of spherulite was measured as a function of time. The growth rate at various T_c was obtained from the slope of the plots of spherulite diameter versus time.

The kinetic data of isothermal crystallization can be analyzed using the spherulitic growth rate in the context of Hoffman-Lauritzen secondary nucleation theory. Accordingly, the growth rate $G(T)$ is given as a function of the crystallization temperature by the following bi-exponential equation[41]:

$$G(T) = G_0 \exp\left[\frac{-U^*}{R(T_c - T_\infty)}\right] \exp\left[\frac{-K_g}{T_c(\Delta T)f}\right] \tag{8}$$

where G_0 is the pre-exponential factor independent of temperature. K_g is a nucleation parameter. The remaining factors have the same meaning as outlined in eq. (7).

If spherulites are assumed to grow in a free space without impingement, the total volume relative to the unit volume transformed by time, t, is given by the following equation[30]:

$$V_{\text{free}} = \sum_{i=1}^{\infty} n_i \left(\frac{4\pi}{3}\right)[G(t - t_i)]^3 \tag{9}$$

where n_i is the number of nuclei per unit volume activated at time, t_i, and G is the radial growth rate. If the mode of nucleation is simultaneous then,

$$V_{\text{free}} = N\left(\frac{4\pi}{3}\right)[G(t)]^3 \tag{10}$$

where N is the number of effective nuclei. For the real space in which a number of spherulites impinge with each other and their growth is restricted, the Avrami-Evans theory proposed,

$$1 - \frac{V}{V_\infty} = \exp(-V_{\text{free}}) \tag{11}$$

where V_∞ is the transformable volume fraction and V is the volume fraction transformed by a certain time. By representing V/V_∞ by the degree of crystallization, $X(t)$, and replacing eq. (10) by Kt^3, eq. (10) was transformed into the following equation:

$$1 - X(t) = \exp(-Kt^3) \tag{12}$$

where

$$N = \frac{3K}{4\pi G^3} \tag{13}$$

From eq. (13), the growth rates combined with the nonisothermal rate constants determined from eqs. (7) and (8), respectively, were used to estimate the number of effective nuclei as a function of temperatures.

RESULTS AND DISCUSSION

Equilibrium melting temperature

The Hoffman-Weeks plots of neat PP, vetiver grass-PP, and rossells-PP composites are shown in Figure 1. The equilibrium melting temperature (T_m^0) of neat PP, vetiver grass-PP, and rossells-PP composites obtained from the Hoffman-Weeks plot is listed in

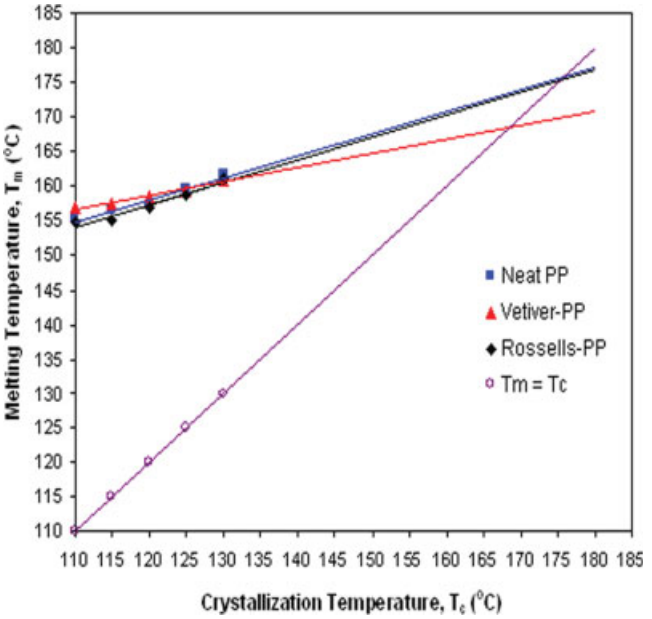

Figure 1 Hoffman-Weeks plots of neat PP and natural fibers-PP composites. [Color figure can be viewed in the online issue, which is available at www.interscience.wiley.com.]

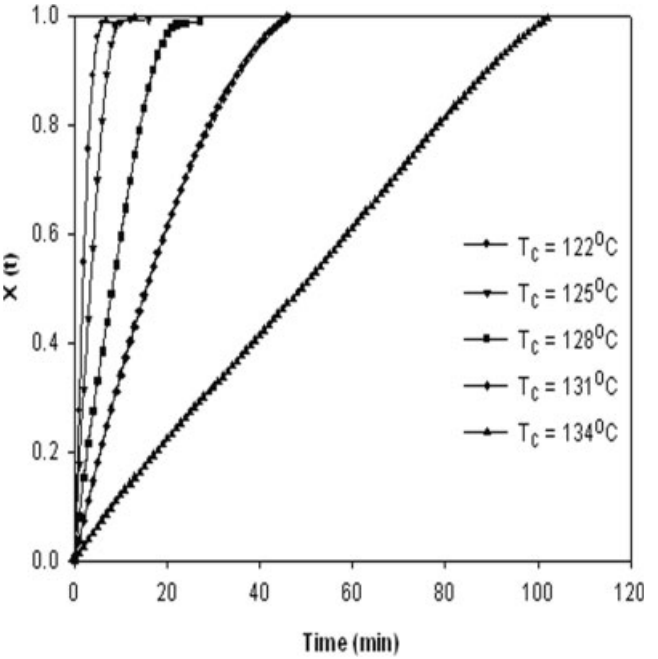

Figure 2 Relative crystallinity ($X(t)$) of neat PP at various crystallization temperatures.

Table I. The addition of natural fibers to PP caused a decrease in T_m^0. This may be due to the presence of natural fibers in the composite, leading to the formation of unstable as well as less perfect spherulites. It can be observed that vetiver grass-PP composite exhibited lower T_m^0 than rossells-PP composites. Lopez-Manchado and Arroyo[11] also found that the addition of synthetic fibers to PP resulted in a decrease of T_m^0. Additionally, Arroyo et al.[9] has reported that adding more than 10% of glass fiber into the PP composites resulted in decreasing T_m^0 of the composites.

Isothermal crystallization kinetics

Plots of relative crystallinity at various crystallization temperatures of neat PP, vetiver grass-PP, and rossells-PP composites were displayed in Figures 2–4, respectively. Half-time of crystallization obtained from the time by which the relative degree of crystallization reached the value of 0.5 was shown in Figure 5. As expected, the half-time of crystallization increased when the crystallization temperature increased. It can be seen that the composites showed a noticeable decrease in half-time of crystallization when compared to that of neat PP. This may be attributed to the nucleating effect of the natural fibers on PP crystallization. Moreover, rossells-PP composite gave the lower half-time of crystallization than vetiver grass-PP composite.

In addition, the relative degree of crystallinity shown in Figures 2–4 was used to determine Avrami

TABLE I
Equilibrium Melting Temperature (T_m^0) of Neat PP, Vetiver Grass-PP, and Rossells-PP Composites

Samples	T_m^0 (°C)
Neat PP	179.03
Vetiver-PP	168.42
Rossells-PP	175.34

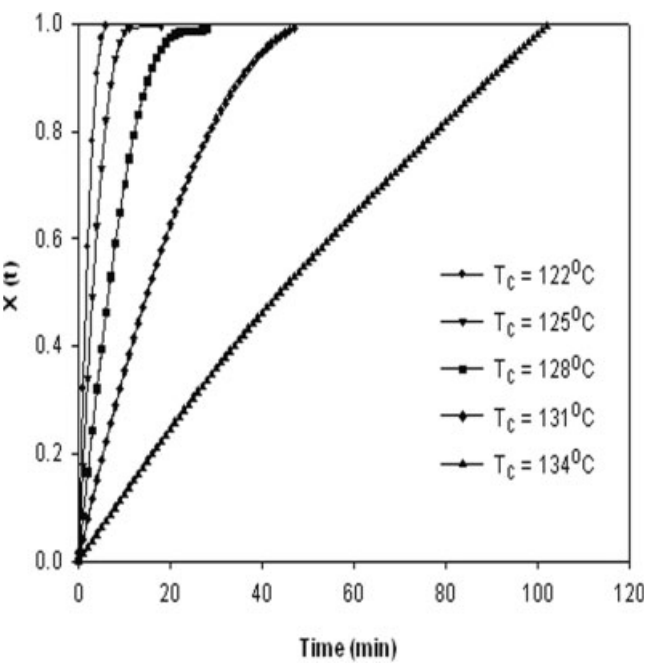

Figure 3 Relative crystallinity ($X(t)$) of vetiver grass-PP composite at various crystallization temperatures.

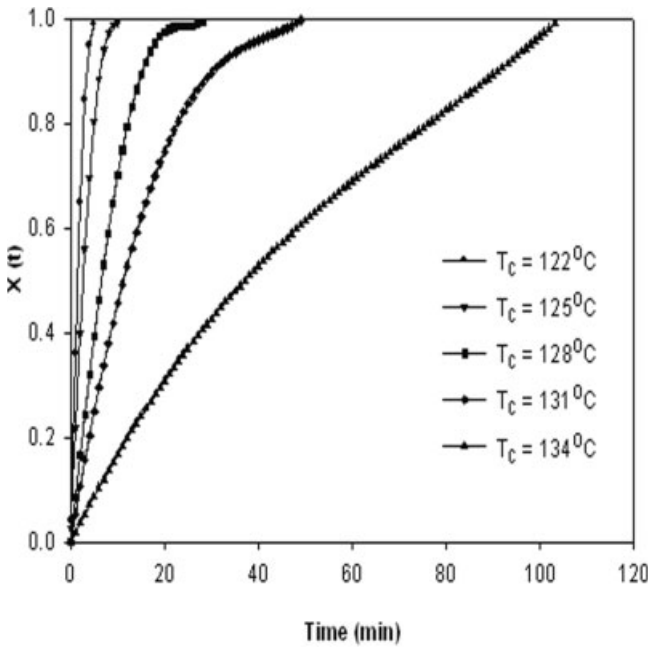

Figure 4 Relative crystallinity ($X(t)$) of rossells-PP composite at various crystallization temperatures.

exponent (n) using Avrami equation (eq. (2)). The plots of Avrami exponent of neat PP, vetiver grass-PP, and rossells-PP composites are illustrated in Figure 6. The Avrami exponent of neat PP was in a range of 1.57 to 2.66. The natural fiber-PP composites had lower n values than that of neat PP. Both vetiver grass-PP and rossells-PP composites showed n values in the same ranges, 1.21–1.32. In this study, it was observed that all Avrami exponents were noninteger values. The difference of n values may attribute to the secondary crystallization process, complex nucleation modes, and the change in the material density. Moreover, a study of cellulose-thermoplastic composites by Quillen et al. has shown that the presence of a transcrystalline layer (TCL) changes the n exponent obtained from the Avrami analysis.[42] In their study, the change in n value related to the change in shape of crystallites because of changes in nuclei concentration with the inclusion of cellulose fiber. For the heterogeneous nucleation case, the shape lies between a diffusion-controlled sphere ($n = 3.0$) and a truncated sphere ($n = 1.5$).[20] The addition of natural fibers tended to push the crystallites towards the truncated shape. This shift was likely resulted from the increased nucleation sites on the fiber surface, but not from a change in the crystal growth. The increased nuclei concentration caused the impinging nuclei to truncate instead of completing spherulitic structures.

The half-time of crystallization in Figure 5 was used to calculate the isothermal rate constant according to eq. (4). Also, the relative degree of crystallinity in Figures 2–4 was used to determine crystallization rate constant from Avrami equation referring to eq. (2). The isothermal rate constant from half-time of crystallization and from Avrami plot as a function of crystallization temperature are shown in Figure 7. It was observed that the isothermal crystallization rate constant decreased when the crystallization temperature increased. Additionally, the rate constants of the composites obtained from both Avrami plot and half-time of crystallization were higher than those of neat PP. When compared between natural fiber-PP composites, rossells-PP composite showed the higher rate constant than vetiver grass-PP composite. This result was in good agreement with the lower half-time of crystallization of rossells-PP composite as previously mentioned. Lopez-Manchado and Arroyo[11] have also observed that the addition of synthetic fibers to PP resulted in the higher rate of crystallization. They have reported that both unmodified and modified synthetic fibers led to the rise in rate of crystallization because of the nucleating effect of fibers on PP crystallization. In case of the modified fibers, they suggested that the better affinity between the fibers and polymer matrix was owing to the higher nucleating effect of the fibers.

To compare the rate constants obtained from the Avrami plot and half-time of crystallization, the isothermal rate constants were converted to nonisothermal rate constants by eq. (6). The nonisothermal rate constant derived from both methods are presented in Figure 8. The result from the plots showed that the nonisothermal rate constant obtained from Avrami plots and half-time of crystallization was not signifi-

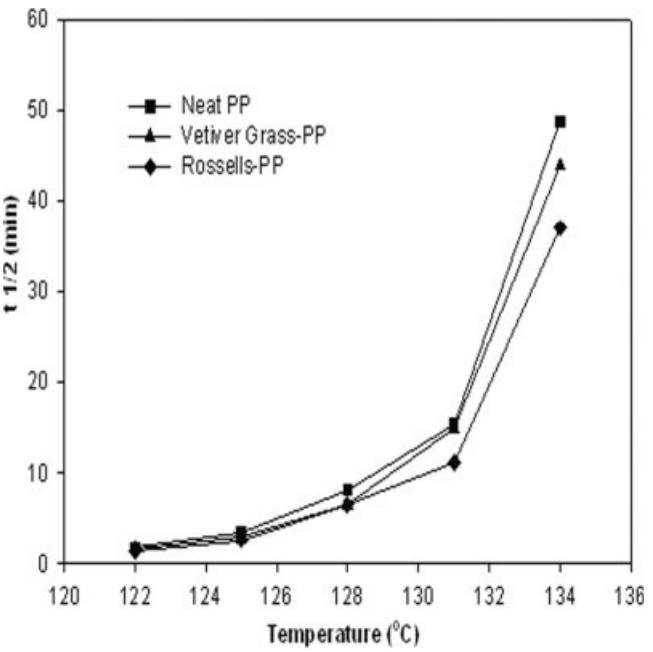

Figure 5 Half-time of crystallization ($t_{1/2}$) as a function of crystallization temperatures for neat PP and natural fiber-PP composites.

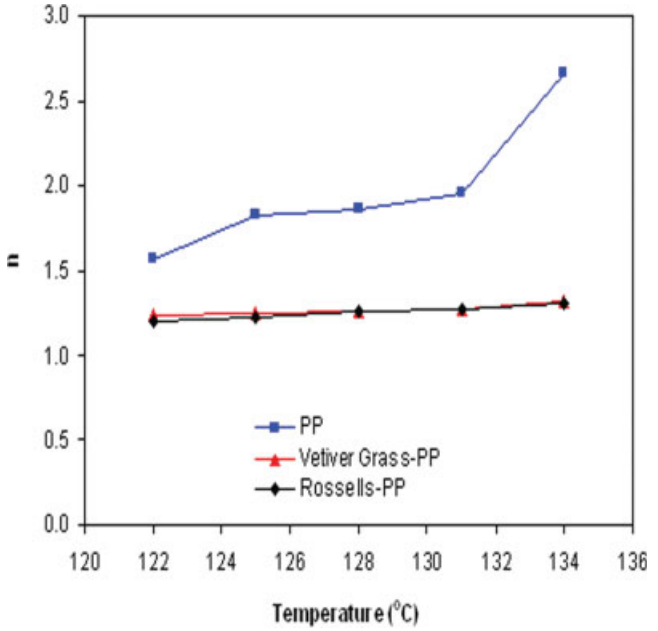

Figure 6 Avrami exponent (n) as a function of crystallization temperatures for neat PP and natural fiber-PP composites. [Color figure can be viewed in the online issue, which is available at www.interscience.wiley.com.]

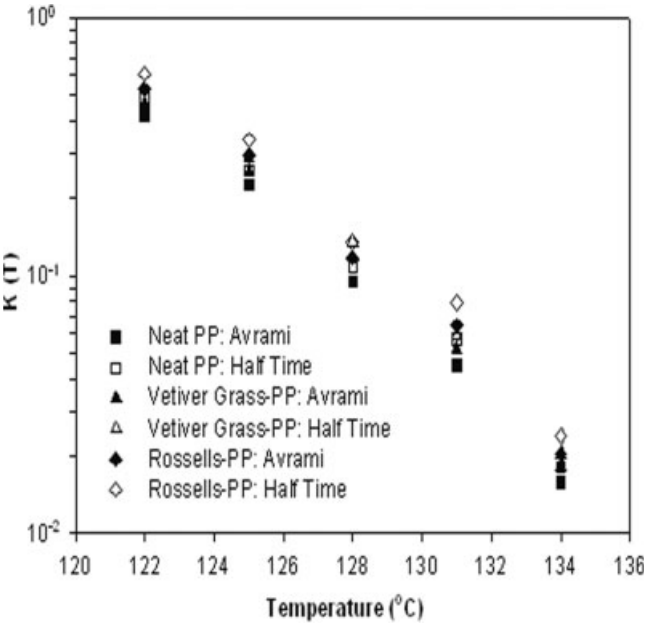

Figure 8 Nonisothermal rate constant, $K(T)$, from half-time crystallization and Avrami plot as a function of crystallization temperature for neat PP and natural fiber-PP composites.

cantly different. Therefore, assuming an Avrami exponent of 3.0 and calculating the isothermal rate constant by eq. (3) seems to be valid for neat PP and natural fiber-PP composites.

The nonisothermal rate constant from half-time of crystallization obtained from Figure 8 was then fitted to eq. (7) to obtain the nonisothermal rate constant in a wide range of crystallization temperatures of neat PP and natural fiber-PP composites as illus-

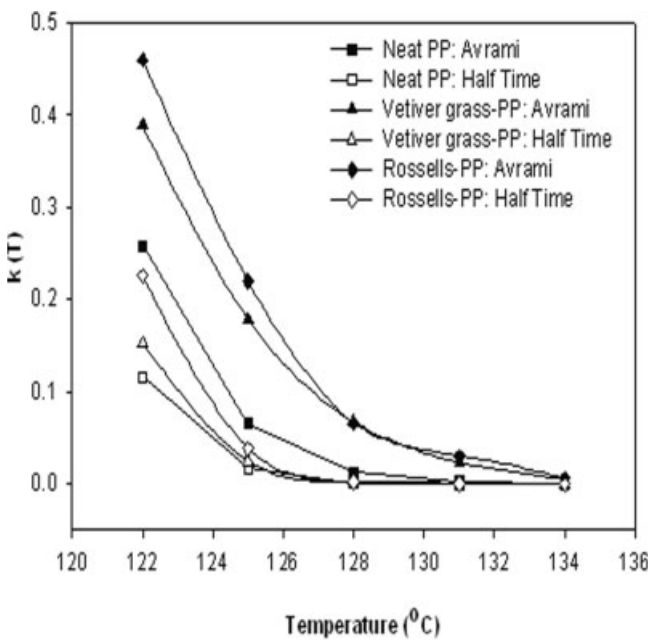

Figure 7 Isothermal rate constant, $k(T)$, from half-time of crystallization and from Avrami plot as a function of crystallization temperatures for neat PP and natural fiber-PP composites.

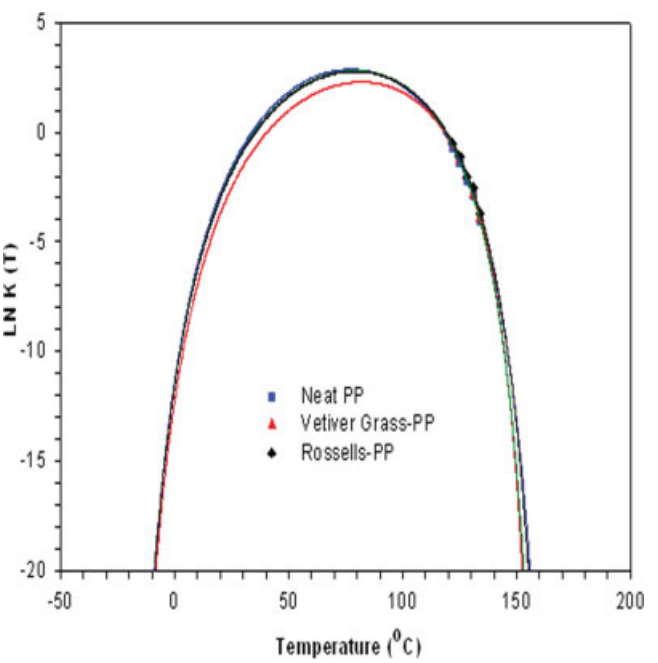

Figure 9 Nonisothermal crystallization rate constants of neat PP and natural fiber-PP composites as a function of crystallization temperature. Symbols represent experimental data while lines indicate the fitting to Hoffman-Lauritzen expression, eq. (7). [Color figure can be viewed in the online issue, which is available at www.interscience.wiley.com.]

TABLE II
Hoffman-Lauritzen Fitted Parameters for Nonisothermal Rate Constants

Samples	K_k (K^2)	$\left(\frac{1}{t_{1/2}}\right)_0$
Neat PP	3.60×10^5	1.98×10^9
Vetiver-PP	2.17×10^4	2.24×10^7
Rossells-PP	3.00×10^4	3.52×10^8

trated in Figure 9. The fitting parameters for nonisothermal rate constants (K_k and $(1/t_{1/2})_0$), which were determined from eq. (7), are summarized in Table II. The nonisothermal rate constant in the wide range of crystallization temperature would be combined with the growth rate to determine the number of effective nuclei, which would be discussed in the next section.

Spherulitic growth rate and transcrystallization

Examples of optical micrographs of crystallized PP in the bulk and on vetiver fiber taken during crystallization process at T_c = 131°C are shown in Figures 10 and 11, respectively. Spherulitic growth rate of PP in the bulk was determined by measuring diameter of spherulites against time as the crystallization isothermally proceeded. Growth rate of transcrystallization (TC) on the fiber surface was evaluated by measuring a width of the TC region perpendicularly to the fiber surface as a function of time. From the spherulitic growth rate study, it was observed that

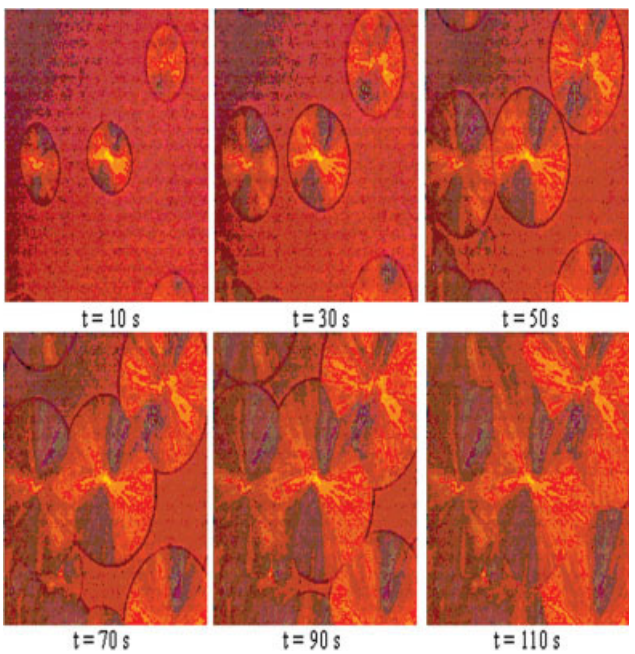

Figure 10 Examples of optical micrographs of crystallized PP in the bulk taken during the crystallization process at T_c = 131°C. [Color figure can be viewed in the online issue, which is available at www.interscience.wiley.com.]

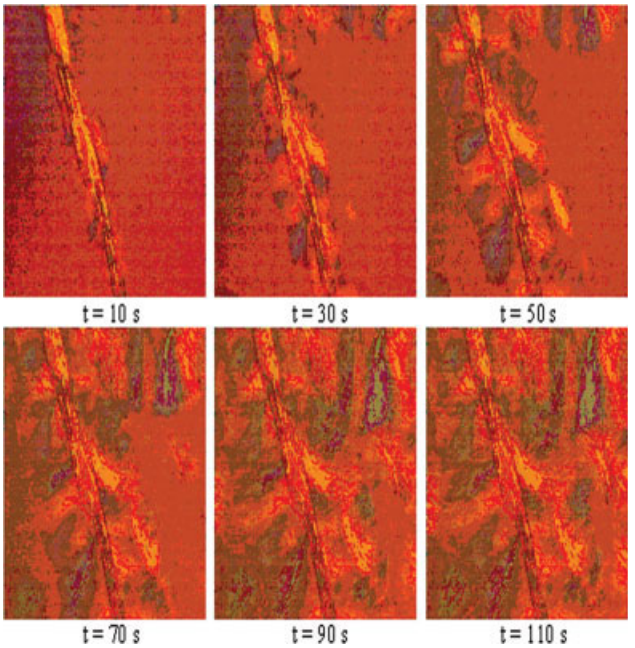

Figure 11 Examples of optical micrographs of TC of PP on vetiver grass fiber taken during the crystallization process at T_c = 131°C. [Color figure can be viewed in the online issue, which is available at www.interscience.wiley.com.]

embedding natural fiber into the polymer melt the fibers may act as nucleating sites for the spherulitic growth as well. As a result, the growing spherulites would be restricted in the lateral direction so that a columnar layer, known as transcrystalline region, was developed on the fiber surface as seen in Figure 11. The TC is possible if the energetic conditions of nucleation are more favorable on the fiber surface than in the bulk of the melt.[43] The growth of TC perpendicularly proceeded to the fiber until the growing front impinged with other spherulites nucleated in the bulk. The mechanism which TC layers occur was not fully understood and there was no rule for predicting the appearance of TC in a particular fiber–matrix system. Besides, its effect on the mechanical properties of the composites and on interfacial properties remained controversial.[44] The ability of cellulose-based fibers such as wood, flax, and sisal to induce transcrystallinity in PP composites has been reported.[19,20,45–47]

The experimental data of spherulitic growth rate of PP in the bulk and transcrystalline region were represented as filled and unfilled symbols in Figures 12 and 13, respectively. From Figure 12, in a case of the bulk, it was found that the growth rate of neat PP was noticeably higher than those of natural fiber-PP composites. This may be due to the restriction of the natural fiber on crystallization process. The growth rate of PP in the bulk of vetiver grass-PP composites was not much different from that of

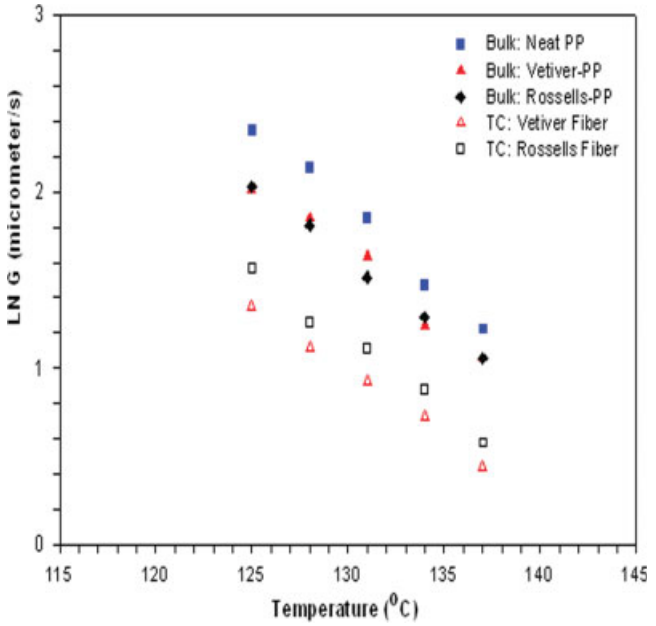

Figure 12 Experimental growth rates of crystallized PP in the bulk and transcrystalline region as a function of crystallization temperatures. [Color figure can be viewed in the online issue, which is available at www.interscience.wiley.com.]

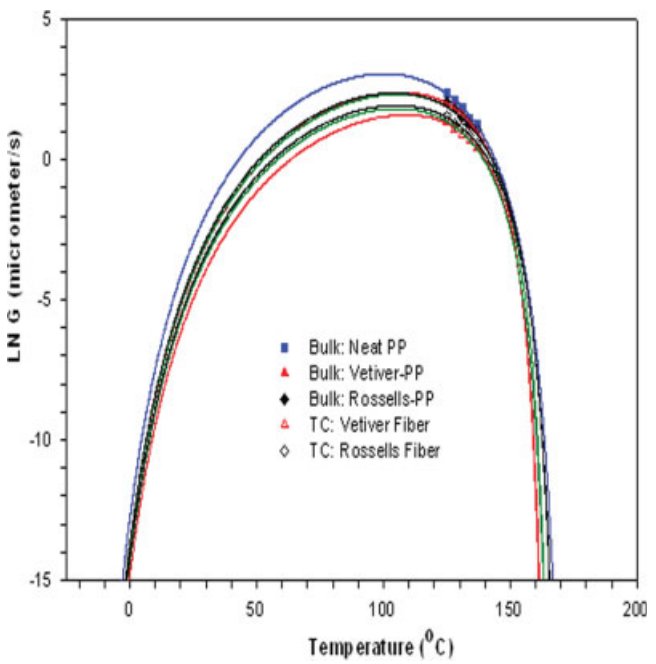

Figure 13 Growth rates of crystallized PP in the bulk and transcrystalline region as a function of crystallization temperatures. Filled symbols represent experimental data obtained in the bulk, and unfilled symbols indicate experimental data obtained on the fiber (TC). Lines refer to fitting to the Hoffman-Lauritzen growth equation, eq. (8). [Color figure can be viewed in the online issue, which is available at www.interscience.wiley.com.]

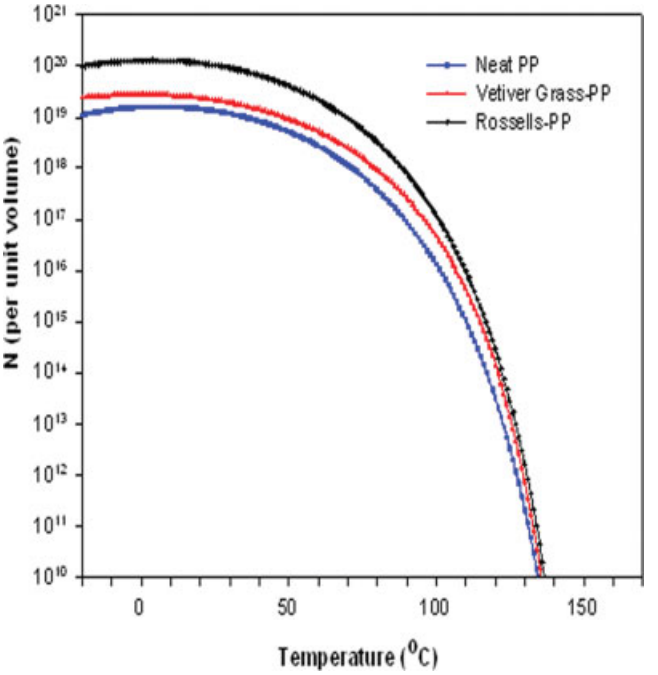

Figure 14 Number of effective nuclei (N) as a function of crystallization temperature for neat PP and natural fiber-PP composites calculated according to eq. (13). [Color figure can be viewed in the online issue, which is available at www.interscience.wiley.com.]

rossells-PP composite. In addition, it was observed that the growth rate of crystallized PP in the bulk of all samples were greater than that of crystallized PP in TC region. When comparing between natural fiber-PP composites, rossells-PP composite had the higher growth rate in the TC region than vetiver grass-PP composite. This implied that the fiber topography of rossells fiber was more favorable for the nucleation of TC than that of vetiver grass. In addition, TC strongly depended on thermodynamic condition such as crystallization temperature or cooling rate because of its nucleation-controlled process.

The experimental spherulitic growth rates at various T_c were then fitted to eq. (8) as shown in Figure 13. It can be verified that the eq. (8) used for determining the spherulitic growth rate in the bulk could also be applied to the growth rate in TC region in this study. The fitting parameters for the spherulitic growth rate, K_g and G_0, in the bulk and in TC region were elucidated and then listed in Tables III and IV, respectively.

TABLE III
Nucleation Constant (K_g) and Pre-exponent Factor (G_0) of Neat PP and Natural Fiber-PP Composites is Bulk

Sample	K_g (K^2)	G_0 (m/s)
Neat PP	1.32×10^5	8.82×10^{-1}
Vetiver-PP	6.88×10^4	5.90×10^{-2}
Rossells-PP	9.89×10^4	1.50×10^{-1}

TABLE IV
Nucleation Constant (K_g) and Pre-exponent Factor (G_0) of Neat PP and Natural Fiber-PP Composites in TC Region

Sample	K_g (K^2)	G_0 (m/s)
Vetiver-PP	6.22×10^4	1.95×10^{-2}
Rossells-PP	9.43×10^4	8.00×10^{-2}

From Tables III and IV, it was found that both K_g of natural fiber-PP composites in bulk and transcrystalline region were lower than that of neat PP in the bulk. It is well known that a foreign surface frequently reduces the nucleus size needed for crystal growth. This is because the creation of the interface between polymer crystal and substrate may be less hindered than the creation of the corresponding free polymer crystal surface. A heterogeneous nucleation path makes use of a foreign pre-existing surface to reduce the free energy opposing primary nucleation.[29] Additionally, it revealed that the G_0 of natural fiber-PP composites were lower than that of neat PP. According to a study by Wang et al.,[27] it has been observed that the incorporation of the $BaSO_4$ into PP caused a decrease of free volume available for PP chains to move, which certainly resulted in a decrease in G_0. Moreover, the interfacial modification improved the adsorption effects of macromolecular chains on particle surface, which resulted in an addition barrier for the motion of the macromolecules. This situation is quite similar to the polymer matrix with very high molecular weight, leading to very high entanglement density. Therefore, a decrease in G_0 with improved interfacial adhesion is possibly due to retardant mechanism similar to the molecular weight dependence of G_0.

From Figure 13, it was found that growth rates of both neat PP and natural fiber-PP composites were represented by a bell-shaped curve as a function of temperature. The spherulitic growth rates combined with the nonisothermal rate constants determined by eqs. (7) and (8), respectively, were used to estimate the number of effective nuclei as a function of temperature. Figure 14 displays the number of effective nuclei as a function of crystallization temperature for neat PP and natural fiber-PP composites according to eq. (13). Typically, the number of effective nuclei decreased with increasing T_c. It was seen that the number of effective nuclei of natural fiber-PP composites was higher than that of neat PP. Moreover, rossells-PP composite showed the highest number of effective nuclei. This result gave good corresponding to the highest growth rate in the TC region of rossells-PP composite as discussed earlier.

Generally, the rate of crystallization depends on both nucleation rate and growth rate. In this study, it was found that the growth rate of the composites were lower than that of neat PP. However, the higher rate of crystallization of the composites than that of neat PP was observed. This implied that the nucleation rate dominated the growth rate. Furthermore, it appeared that the number of effective nuclei of natural fiber-PP composites was higher than that of neat PP. This suggested that natural fibers may act as nucleating agents in the composites. Wang and Hwang[48] have shown that fiber topography, chemical compositions of the surface, and surface energy influenced the nucleation on the fiber surface. From our experimental observations it was interesting to point out that both natural fibers used in this study have α-nucleating ability. Varga and Karger-Kocsis[49] also reported that the high-modulus carbon fiber has strong α-nucleation ability in quiescent PP melt. On the other hand, there are several additives using in PP melt having β-nucleating efficiency.[50,51]

However, it is worth to mention that the number of effective nuclei strongly depends on the fitting parameters of rate constant equation (according to Table II) and growth rate equation (according to Table III). For the fact that the low crystallization temperatures or very high cooling rates cannot be achieved in the DSC and the spherulitic growth rate experiments; therefore, the fitting of number of effective nuclei at the low temperature range may not be very accurate. At this range, some errors might be introduced in the prediction of the number of effective nuclei at very low temperature range.

CONCLUSIONS

From this study it can be concluded that natural fibers i.e., vetiver grass and rossells, affected the crystallization of PP in the composites. A decrease in equilibrium melting temperature, half-time of crystallization, and an increase in the rate of crystallization were observed in the PP composites when compared to those of neat PP. The presence of natural fibers in the composites led to a decrease in Avrami exponent, which indicated that the fibers tended to cause impinging nuclei and led to truncated spherulitic shapes. Moreover, the decrease in Avrami exponent was probably due to the development of TC. Transcrystallinity growth of PP could be seen on the fiber surfaces. According to an increase in the number of effective nuclei when natural fibers were incorporated into PP matrix, it can be suggested that natural fibers could serve as nucleating agents in the composites. Additionally, it was found that rossells-PP composite had the lowest half-time of crystallization resulting in the highest rate of crystallization. In addition, rossells-PP composite gave the highest growth rate in transcrystalline region. Also, the number of effective nuclei of rossells-PP composites was higher than that of vetiver grass-PP composites.

The authors thank the NEP Realty and Industry Public Co., Ltd., for donating rossells fiber, and the Land Development Department (LDD), Nakorn Ratchasima, Thailand for supplying vetiver grass.

References

1. Sinha, R. S.; Okamoto, M. Prog Polym Sci 2003, 28, 1539.
2. Bledzki, A. K.; Gassan, J. Prog Polym Sci 1999, 24, 221.
3. Schuh, T. G. Available at http://www.ienica.net/fiberseminar/schuh.pdf.
4. Bruijn, J. C. M. Appl Compos Mater 2000, 7, 415.
5. Ruksakulpiwat, Y.; Suppakarn, N.; Sutapun, W.; Thomthong, W. Compos A 2007, 38, 590.
6. Saheb, D. N.; Jog, J. P. Adv Polym Technol 1999, 18, 351.
7. Wambua, P.; Ivens, J.; Verpoest, I. Compos Sci Technol 2003, 63, 1259.
8. Mohanty, A. K.; Misra, M.; Hinrichsen, G. Macromol Mater Eng 2000, 276/277, 1.
9. Arroyo, M.; Lopez-Manchado, M. A.; Avalos, F. Polymer 1997, 38, 5587.
10. Avalos, F.; Lopez-Manchado, M. A.; Arroyo, M. Polymer 1998, 39, 6173.
11. Lopez-Manchado, M. A.; Arroyo, M. Polymer 1999, 40, 487.
12. Lopez-Manchado, M. A.; Biagiotti, J.; Torre, L.; Kenny, J. M. Polym Eng Sci 2000, 40, 2194.
13. Arroyo, M.; Zitzumbo, R.; Avalos, F. Polymer 2000, 41, 6351.
14. Wang, C.; Liu, C. R. Polymer 1997, 38, 4715.
15. Wang, C.; Liu, C. R. Polymer 1999, 40, 289.
16. Wang, C.; Hwang, L. M. Polymer 1996, 34, 1435.
17. Saujanya, C.; Radhakrishnan, S. Polymer 2001, 42, 4537.
18. Cyras, V. P.; Kenny, J. M.; Vazquez, A. Polym Eng Sci 2001, 41, 1521.
19. Zafeiropoulos, N. E.; Baillie, C. A.; Matthews, F. L. Compos A 2001, 32, 525.
20. Harper, D.; Wolcott, M. Compos A 2004, 35, 385.
21. Pracella, M.; Chionna, D.; Kulinski, Z.; Piorkowska, E. Compos Sci Technol 2006, 66, 2218.
22. Menczel, J.; Varga, J. J Therm Anal 1983, 28, 161.
23. Mucha, M.; Marszalek, J.; Findrych, A. Polymer 2000, 41, 4137.
24. Maiti, P.; Nam, P. H.; Okamoto, M.; Hasegawa, N.; Usuki, A. Macromolecules 2002, 35, 2042.
25. Strawhecker, K. E.; Manias, E. Chem Mater 2003, 15, 844.
26. Kim, S. H.; Ahn, S. H.; Hirai, T. Polymer 2003, 44, 5625.
27. Wang, K.; Wu, J.; Zeng, H. Eur Polym J 2003, 39, 1647.
28. Esteves, A. C. C.; Barros-Timmons, A. M.; Martins, J. A.; Zhang, W.; Cruz-Pinto, J.; Trindade, T. Compos B 2005, 36, 51.
29. Papageorgiou, G. Z.; Achillias, D. S.; Bikiaris, D. N.; Karayannidis, G. P. Therm Acta 2005, 427, 117.
30. Nagasawa, S.; Fujimori, A.; Masuko, T.; Iguchi, M. Polymer 2005, 46, 5241.
31. Nitta, K. H.; Asuka, K.; Liu, B.; Terano, M. Polymer 2006, 47, 6457.
32. Kowalewski, T.; Galeski, A. J Appl Polym Sci 1986, 32, 2919.
33. Ruksakulpiwat, Y.; Kluensamrong, K.; Somnuk, U.; Sutapun, W.; Suppakarn, N. 31st Congress on Science and Technology of Thailand 2005, E0026.
34. Avrami, M. J Chem Phys 1939, 7, 1103.
35. Avrami, M. J Chem Phys 1940, 8, 212.
36. Avrami, M. J Chem Phys 1941, 9, 177.
37. Nakamura, K.; Watanabe, T.; Katayama, K.; Amano, T. J Appl Polym Sci 1972, 17, 1077.
38. Nakamura, K.; Katayama, K.; Amano, T. J Appl Polym Sci 1973, 17, 1031.
39. Isayev, A. I.; Churdpunt, Y.; Guo, X. Int Polym Process 2000, 15, 72.
40. Advance Thermal Analysis System (ATHAS Databank). Available at http://web.utk.edu/athas/edu.
41. Hoffman, J. D.; Davis, G. T.; Lauritzen, L. I. In Treatise on Solid State Chemistry: Crystalline and Non-crystalline Solids; Hannay, J. B., Ed.; Plenum: New York, 1976; Vol. 3, Chapter 7.
42. Quillen, D. T.; Caulfield, D. F.; Koutsky, J. A. J Polym Sci Part B: Polym Phys 1994, 52, 605.
43. Varga, J. In Polypropylene: Structure Blends and Composites; Karger-Kocsis, J. Ed.; Chapman & Hall: London, 1995; Vol. 1.
44. Quan, H.; Li, Z.; Yang, M.; Huang, R. Compos Sci Technol 2005, 65, 999.
45. Joseph, P. V.; Joseph, K.; Thomas, S.; Pillai, C. K. S.; Prasad, V. S.; Groeninckx, G.; Sarkissova, M. Compos A 2003, 34, 253.
46. Arbelaiz, A.; Fernández, B.; Ramos, J. A.; Mondragon, I. Therm Acta 2006, 440, 111.
47. Amash, A.; Zugenmaier, P. Polymer 2000, 41, 1589.
48. Wang, C.; Hwang, L. M. J Polym Sci Part B: Polym Phys 1996, 34, 47.
49. Varga, J.; Karger-Kocsis, J. Polymer 1995, 36, 4877.
50. Varga, J. J Macromol Sci Phys 2002, 41, 1121.
51. Mi, Y.; Chen, X.; Guo, Q. J Appl Polym Sci 1997, 64, 1267.